

Morphology of Critical Nuclei in Solid-State Phase Transformations

Lei Zhang*

Department of Mathematics, Penn State University, Pennsylvania 16802, USA

Long-Qing Chen[†]

Department of Materials Science and Engineering, Penn State University, Pennsylvania 16802, USA

Qiang Du[‡]

Department of Mathematics and Materials Science and Engineering, Penn State University, Pennsylvania 16802, USA

(Received 6 January 2007; published 28 June 2007)

Predicting the shape of a critical nucleus in solids has been a long-standing problem in solid-state phase transformations. We show that a diffuse-interface approach together with a minimax algorithm is able to predict the critical nucleus morphology in elastically anisotropic solids without *a priori* assumptions. We demonstrate the possibility of nonconvex surfaces for critical nuclei. It is found that strong elastic energy contributions may lead to critical nuclei whose point group symmetry is below the crystalline symmetries of both the new and the parent phases.

DOI: [10.1103/PhysRevLett.98.265703](https://doi.org/10.1103/PhysRevLett.98.265703)

PACS numbers: 64.60.Qb

Nucleation is perhaps the most common physical phenomenon in nature. It takes place when a material becomes metastable with respect to its transformation to a new state (solid, liquid, and gas) or new crystal structure. Much of our current understanding of nucleation owes to the classical nucleation theories developed in 1930s. Early nucleation theories mostly considered phase changes in fluids, e.g., a liquid droplet in a vapor phase, and naturally assumed spherical shapes for the critical nuclei. The thermodynamic properties of a nucleus are assumed to be the same as in the corresponding bulk. The size of a critical nucleus is then determined as a result of bulk free energy reduction and interfacial energy increase $r = -2\gamma/\Delta G_v$, where γ is the interfacial energy per unit area between a nucleus and the parent matrix, and ΔG_v is the free energy driving force per unit volume. Despite the assumption of spherical shapes for critical nuclei, the same classical theories have been utilized to interpret kinetics of many phase transformations involving solids including solid to solid transformations. For some systems, the classical nucleation theory has been shown to provide a good description of the nucleation kinetics.

It has long been recognized that, in general, nucleation in solids can be significantly more complicated than that in fluids. First of all, due to the crystallographic nature of most solids, the interfacial energy between a nucleus and the matrix is generally anisotropic, and thus the minimum surface shape is nonspherical. Second, the lattice parameters of a new phase and the corresponding parent are typically different, so elastic energy is generated during nucleation to accommodate the lattice mismatch between a nucleus and the matrix. The shape of a critical nucleus in the presence of interfacial energy anisotropy alone can be deduced from the well-known Wulff construction. However, predicting the shape of a critical nucleus in the

presence of both elastic energy and surface energy anisotropy is particularly challenging, since elastic energy contribution depends on the morphology of a nucleus and lattice mismatch between the nucleus and the matrix.

Prior applications of classical nucleation theory to solid-state transformations typically assume the shape of a nucleus as an *a priori* and include the elastic energy contribution to nucleation as an extra nucleation barrier, i.e., the size of a nucleus $a^* \sim -\beta^* \gamma (\Delta f_v + E_e)^{-1}$, where β^* is a numerical factor depending on the shape of the nucleus, Δf_v is the bulk driving force for nucleation, and E_e is the elastic strain energy contribution to nucleation on the order of $C\epsilon_0^2$, where C is the elastic modulus and ϵ_0 is the lattice mismatch strain (transformation strain, eigenstrain, stress-free strain) between the nucleus and matrix. For example, Brenner, Iordanskii, and Marchenko [1] studied the kinetics of nucleation and growth of a new phase in a solid. They assumed an oblate shape of nuclei, which reduces the elastic energy arising from the lattice accommodation between the new phase and matrix.

In this Letter, we propose a nonclassical approach to nucleation in solids by integrating a diffuse-interface phase-field description [2] and a minimax variational approach [3]. It is then applied to predict the critical nucleus morphology in the presence of anisotropic interfacial energy and/or anisotropic elastic interactions. Our focus here is on the nucleus morphology rather than the nucleation rate or kinetics. This problem is quite different from the saddle-point search when a solid is homogeneously transformed to a new phase throughout the system, described by a homogeneous free energy as a function of a homogeneous order parameter.

Following the seminal work by Cahn and Hilliard [4], the nonclassical theory has been previously applied to nucleation in solids; for example, Roy *et al.* [5] discussed

the nucleation in the presence of a general long-range interaction, focusing on the critical order parameter profiles rather than predicting the morphology of a nucleus. Wang and Khachatryan [6] examined the morphology of nuclei during a martensitic transformation by switching on and off Langevin noise, and the particles obtained using this approach do not necessarily correspond to saddle-point configurations associated with a critical nucleus. Poduri and Chen [7] studied the nucleation of an ordered precipitate from a disordered matrix by extending the diffuse-interface theory of Cahn and Hilliard. Chu *et al.* [8] explored the nucleation of martensites using a diffuse-interface phase model. More recently, Gagne *et al.* [9] studied the morphological evolution using Langevin simulations of martensitic transformations in two dimensions. They concluded that systems with long-range interactions quenched into a metastable state near the pseudospinodal exhibit nucleation that is qualitatively different from the classical nucleation near the coexistence curve. It is noted that all existing diffuse-interface theories for nucleation in solids ignore the anisotropic interfacial energy and anisotropic long-range elastic interactions.

Without loss of generality, we consider a structural transition with no compositional changes. We assume that the structural difference between the parent phase and the nucleating phase can be sufficiently described by a single order parameter η . At a given temperature, the free energy dependence on η is described by a double-well potential $f(\eta) = -\eta^2/2 + \eta^4/4 - \lambda h(\eta)$ with wells at $\eta = \pm 1$, $h(\eta) = (3\eta - \eta^3)/2$ so that 2λ determines the well depth difference, i.e., the bulk free energy driving

force for phase transformation from the $\eta = -1$ state to the $\eta = 1$ state.

The total free energy of an inhomogeneous system described by a spatial distribution of η is given by

$$E = \int_{\Omega} \left(f(\eta) + \frac{\alpha}{2} |\nabla \eta|^2 \right) d\mathbf{x},$$

where the gradient energy coefficient α is a constant in Ω for isotropic interfacial energy. For illustration, we take $\Omega = (-1, 1)^d$ in this Letter with d being the space dimension.

If the interfacial energy is anisotropic, as usually is the case for nucleation in solids, either the gradient energy coefficient can be expressed as a second or higher order derivative or, rather artificially but common in the phase-field models, it is made directionally dependent. To incorporate the effect of long-range elastic interactions on the morphology of a critical nucleus, and thus the nucleation barrier, the computation of the elastic energy E_e is needed for any arbitrary distribution of η . We hereby assume that the elastic modulus is anisotropic but homogeneous, so we may employ the microscopic elasticity theory of Khachatryan [10]. For a cubic crystal,

$$E_e = \frac{1}{2(2\pi)^d} \int_{\hat{\Omega}} d\mathbf{k} B(\mathbf{n}) |\hat{\eta}(\mathbf{k})|^2, \quad (1)$$

which is over the reciprocal space $\hat{\Omega}$ of the reciprocal lattice vector \mathbf{k} , $\mathbf{n} = \mathbf{k}/|\mathbf{k}| = (n_1, n_2, n_3)$ is the normalized unit vector, and, in three dimensions,

$$B(\mathbf{n}) = 3(c_{11} + 2c_{12})\epsilon_0^2 - \frac{(c_{11} + 2c_{12})^2 \epsilon_0^2 [1 + 2\zeta s(\mathbf{n}) + 3\zeta^2 n_1^2 n_2^2 n_3^2]}{c_{11} + \zeta(c_{11} + c_{12})s(\mathbf{n}) + \zeta^2(c_{11} + 2c_{12} + c_{44})n_1^2 n_2^2 n_3^2},$$

where c_{11} , c_{12} , and c_{44} are the elastic constants in the Voigt notation, ϵ_0 is the lattice mismatch between the nucleating new cubic phase and the parent cubic phase, $\zeta = (c_{11} - c_{12} - 2c_{44})/c_{44}$ is the elastic anisotropic factor, and $s(\mathbf{n}) = n_1^2 n_2^2 + n_1^2 n_3^2 + n_2^2 n_3^2$.

Taking into account the long-range elastic interactions and surface energy anisotropy, the increase in the total free energy arising from the order parameter fluctuation in an initially homogeneous state with η_0 is given by

$$\Delta E_{\text{total}} = \int_{\Omega} \left[\delta f(\eta) + \frac{\alpha_x}{2} \left(\frac{\partial \eta}{\partial x} \right)^2 + \frac{\alpha_y}{2} \left(\frac{\partial \eta}{\partial y} \right)^2 \right] d\mathbf{x} + \beta E_e,$$

where $\delta f(\eta) = f(\eta) - f(\eta_0)$ and E_e is given by (1). Rather than varying the magnitudes of lattice mismatch and elastic constants, we use a factor β to study the effect of the relative elastic energy contribution to the chemical driving force on the critical nucleus morphology.

Since nucleation takes place by overcoming the minimum energy barrier, a critical nucleus is defined as the spatial order parameter fluctuation which has the minimum

free energy increase among all fluctuations which lead to nucleation. Therefore, we may find the critical nucleus by computing the saddle point of the energy functional, of the order parameter η , that has the highest energy in the minimum action path. This is consistent with the large derivation theory, which states that the most probable path (that minimizes the action [11]) passes through the saddle point in the large time limit. The usual calculus of variation can be used to derive the Euler-Lagrange equation for the saddle point:

$$\alpha_x \frac{\partial^2 \eta}{\partial^2 x} + \alpha_y \frac{\partial^2 \eta}{\partial^2 y} = \frac{\partial}{\partial \eta} \delta f(\eta) + \frac{\beta}{(2\pi)^d} \times \int_{\hat{\Omega}} B(\mathbf{n}) \hat{\eta}(\mathbf{k}) e^{i\mathbf{k} \cdot \mathbf{x}} d\mathbf{k}.$$

In this Letter, we work with periodic boundary conditions so that Fourier spectral methods can be utilized [2]. Solutions to the above equation lead to all critical points in the energy landscape, including the saddle-point order parameter profiles.

There are various approaches for solving variational problems numerically. While the most notable ones are for finding minimizers, algorithms have also been developed to find minimum energy paths and to search for saddle points [12]. In this work, to ensure the robust solution of a saddle point, we employ an algorithm based on the mountain pass theorem, which adopts the *minimax* technique that has been studied extensively in calculus of variation and optimization [3,13].

The key of the minimax algorithm is to construct a solution submanifold \mathcal{M} so that a local minimum point of ΔE_{total} on \mathcal{M} yields a saddle point. To ensure stability and monotonicity, a steepest descent search is applied to approximate a local minimizer on \mathcal{M} . Meanwhile, to guarantee the convergence of the algorithm, it is imperative to use a *return rule* to prevent the descent search from leaving the submanifold. We follow the approach studied by Li and Zhou [14] which is outlined below: (1) For $k = 0$, take a direction ν_0 at a local minimum η_0 , $\mathcal{M}_0 = \{\eta_0 + \text{span}\{\nu_0\}\}$, and search for a local maximum $w^k := \arg \max_{u \in \mathcal{M}_0} \Delta E_{\text{total}}(u)$. (2) For $k \geq 0$, compute the gradient g^k of ΔE_{total} at w^k . If $\|g^k\|$ is less than some tolerance, stop and output w^k as a critical nucleus; otherwise, go to step 3. (3) For $\mathcal{M}_b^{k+1} = \{\nu^k + \text{span}\{\nu_b^k\}\}$, with ν_b^k being the unit vector in the direction of $\nu^k - b g^k$ and b in $(0, \hat{b}_k)$, solve $p(\nu_b^k) := \arg \max_{u \in \mathcal{M}_b^{k+1}} \Delta E_{\text{total}}(u)$. Then solve $b^* := \arg \min_{0 < b < \hat{b}_k} \Delta E_{\text{total}}[p(\nu_b^k)]$, set $\nu^{k+1} = \nu_b^{k*}$, $w^{k+1} = p(\nu^{k+1})$, update k by $k + 1$, and go to step 2.

For efficiency, a *tanh* function is taken as the initial search direction in step 1. In step 2, the number \hat{b}_k is used to control the step size of the steepest descent search to enhance the stability of the algorithm. An inner product given by the integral of the product of the functions and their gradients is adopted to define the variational gradient g^k , which is again efficiently computed via the Fourier spectral method.

We now present examples of predicted critical nucleus morphologies in cubically anisotropic systems. The simulations were performed on a two-dimensional 128^2 grid which was verified to give well-resolved numerical results.

We first consider the case of interfacial energy anisotropy with $\beta = 0$ in ΔE_{total} . Figure 1 shows critical order parameter profiles without and with interfacial energy anisotropy ($\alpha_y/\alpha_x = 1$ or 3, in the 1st row). The predicted anisotropic profile correctly displays the ellipsoidal direction dependence as one would expect from the interfacial energy anisotropy. Note that, although for a given interfacial energy anisotropy the shape can be determined from the Wulff construction, the proposed diffuse-interface approach is able to predict both the size and the shape of a critical nucleus simultaneously.

Examples of predicted critical profiles in the presence of long-range elastic interactions are also shown in Fig. 1 (2nd row) for $\beta = 0.2, 0.8$, and 1.2 , respectively. Here $\eta_0 = -1$, $\alpha_x = \alpha_y = 4 \times 10^{-4}$, $\lambda = 0.05$, $c_{11} = 250$, $c_{12} = 150$, $c_{44} = 100$, and $\epsilon_0 = 0.01$. We see that long-

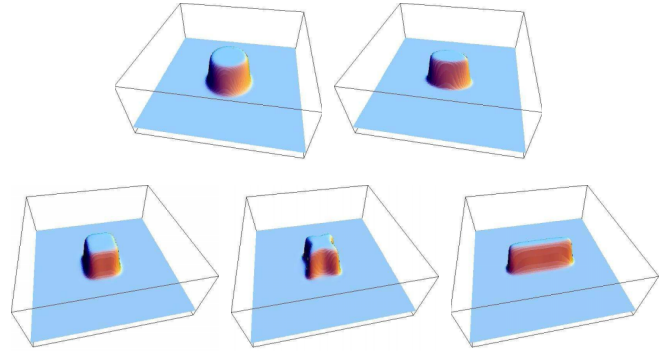


FIG. 1 (color online). Critical nuclei with $\alpha_y/\alpha_x = 1$ or 3 and $\beta = 0$ and cubically anisotropic nuclei with $\beta = 0.2, 0.8$, or 1.2 and $\alpha_y/\alpha_x = 1$.

range elastic interactions can dramatically change the critical nucleus morphology. A strong elastic interaction may lead to critical nuclei with cuboidal, platelike, or even nonconvex shapes (for $\beta = 0.8$). It is emphasized that, although there have been extensive theoretical studies of particle morphologies during growth or coarsening by minimizing the total interfacial and elastic strain energy [15–18], the present work provides a new approach to predict the morphologies of saddle-point critical nuclei without any *a priori* assumptions on the shapes.

To determine the most probable nucleus morphology for a given relative elastic energy and chemical driving force contributions, we plot in Fig. 2 the formation energy of a critical nucleus for different β with $c_{11} = 250$, $c_{12} = 150$, $c_{44} = 200$, but with the same ϵ_0 , λ , α as in Fig. 1. Here the insets contain the contour plots of a number of nucleus profiles as β changes, illustrating the change in the critical nucleus morphology; the small squares and circles are data points based on the computed critical order parameter profiles, and the solid curves are least square fits by cubic

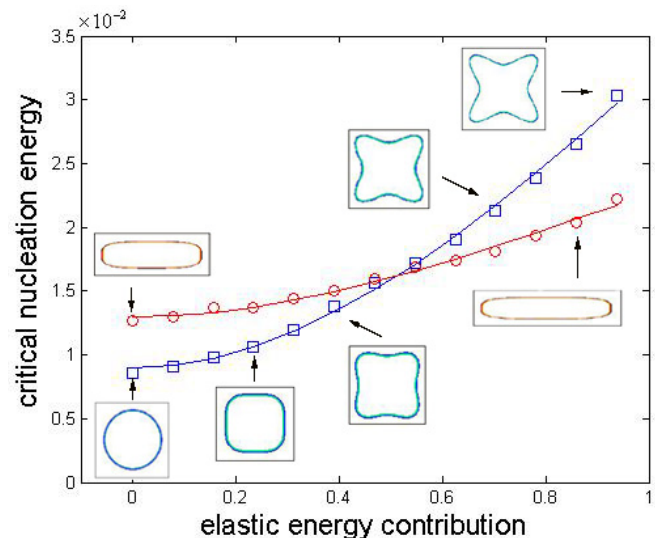


FIG. 2 (color online). Critical nucleation energy with changing elastic energy contribution and critical nuclei profiles.

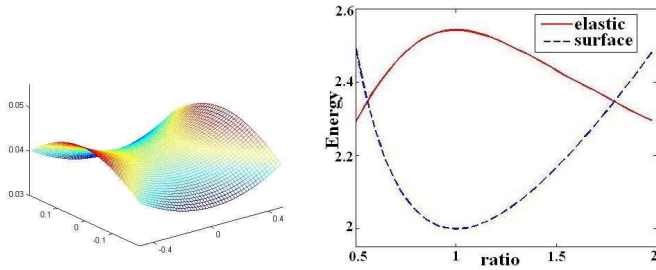


FIG. 3 (color online). Local energy surface near nonconvex nucleus and a comparison of energies for rectangular nuclei.

polynomials. For small β , the critical nucleus with lower energy possesses the symmetry of a cubic crystal, i.e., either nearly circular or square with rounded corners. As β increases to be above 0.35, the nucleus becomes nonconvex. For even larger β (above 0.5), while one saddle-point curve maintains the cubic symmetry, there is a second curve of saddle points with lower energy values corresponding to nuclei having lower symmetry groups. Continuing the latter curve for smaller β below the intersection point shows that it leads to saddle points of higher energy than that for the nonconvex, square, and nearly circular nuclei. Therefore, for intermediate values of β , we find the surprising result of critical nuclei with nonconvex surfaces being the most probable morphology. It should be noted that the present work ignores the possible presence of defects such as dislocations and interfaces, i.e., heterogeneous nucleation.

Thus, we observe that, with a stronger elastic energy contribution, the formation energy for a critical nucleus with a lower symmetry is lower than that with the cubic symmetry but nonconvex interfaces (which are verified to be indeed saddle points, with a 2D illustration of the local energy surface around the nonconvex nucleus given in Fig. 3, where one axis is along the solution direction, and another is along a descent direction). To offer additional understanding on the competition of the elastic and interfacial energies, we compare the energies in Fig. 3 for rectangular nuclei of dimension a by $1/a$ with changing aspect ratios. Taking a sharp interface limit of our diffuse model, i.e., letting η be a Heaviside function with ± 1 inside and outside the rectangle and substituting its Fourier coefficients $\{\hat{\eta}(\mathbf{k}) = \sin(\pi k_x a) \times \sin(\pi k_y / a) / (\pi^2 k_x k_y)\}$ into (1), we get an estimation of the elastic energy (solid red curve), while the sharp surface energy is proportional to $2(a + 1/a)$ (dashed blue curve). It is clear that the surface energy is the smallest for $a = 1$ (thus preferring the cubic symmetry), while the elastic energy is lower with plate shapes. The diffuse-interface model captures this competition and correctly distinguishes the parameter ranges where one energy dominates the other, so that critical nuclei with lower symmetry are

most probable for large elastic energy contributions. It should be noted that, even in two dimensions, there are two equivalent variants for the critical nucleus with a lower symmetry (thus, three variants in three dimensions).

In our calculation, we also observe that, for a fixed β , with the increase of the driving force, the size of critical nuclei reduces and the critical free energy decreases, similar to that predicted from the classical nucleation theory for spherical particles.

In conclusion, we demonstrated in this Letter that the morphology of a critical nucleus or a critical fluctuation in elastically anisotropic solids can be predicted by a combination of the diffuse-interface approach and the minimax algorithm. Our calculations reveal the fascinating possibility of nuclei with nonconvex shapes, as well as the phenomenon of shape bifurcation and the formation of critical nuclei whose symmetry is lower than both the new phase and the original parent matrix.

This work is supported in part by NSF-DMR ITR 0205232 and NSF-DMS 0409297.

*zhang_l@math.psu.edu

†lqc3@psu.edu

‡qdu@math.psu.edu

- [1] E. Brener, S. Iordanskii, and V. Marchenko, Phys. Rev. Lett. **82**, 1506 (1999).
- [2] L. Q. Chen, Annu. Rev. Mater. Res. **32**, 113 (2002).
- [3] P. Rabinowitz, *Minimax Methods in Critical Point Theory with Applications to Differential Equations* (American Mathematical Society, Providence, RI, 1986).
- [4] J. Cahn and J. Hilliard, J. Chem. Phys. **31**, 688 (1959).
- [5] A. Roy *et al.*, Phys. Rev. E **57**, 2610 (1998).
- [6] Y. Wang and A. Khachaturyan, Acta Mater. **45**, 759 (1997).
- [7] R. Poduri and L. Q. Chen, Acta Mater. **44**, 4253 (1996).
- [8] Y. Chu *et al.*, Metall. Mater. Trans. A **31**, 1321 (2000).
- [9] C. Gagne *et al.*, Phys. Rev. Lett. **95**, 095701 (2005).
- [10] A. Khachaturyan, *Theory of Structural Transformations in Solids* (Wiley, New York, 1983).
- [11] R. Kohn, M. Reznikoff, and Y. Tonegawa, Calc. Var. **25**, 503 (2006).
- [12] S. Fischer and M. Karplus, Chem. Phys. Lett. **194**, 252 (1992); I. Ionova and E. Carter, J. Chem. Phys. **98**, 6377 (1993); G. Henkelman, B. Uberuaga, and H. Jonsson, *ibid.* **113**, 9901 (2000).
- [13] J. Moré and T. Munson, Math. Program. **100**, 151 (2004).
- [14] Y. Li and J. Zhou, SIAM J. Sci. Comput. **23**, 840 (2001).
- [15] Y. Wang, L. Q. Chen, and A. G. Khachaturyan, Acta Mater. **41**, 279 (1993).
- [16] S. Conti and B. Schweizer, Arch. Ration. Mech. Anal. **179**, 413 (2006).
- [17] H. Garcke, M. Rumpf, and U. Weikard, Interfaces Free Bound. **3**, 101 (2001).
- [18] X. Li *et al.*, Acta Mater. **52**, 5829 (2004).